Theoretical and Applied Climatology (2019) 138:683–699
https://doi.org/10.1007/s00704-019-02854-4

ORIGINAL PAPER

A model for estimating transpiration of rainfed urban trees in Mediterranean environment

Gianfranco Rana [1] · Rossana M. Ferrara [1] · Gianluigi Mazza [1,2]

Received: 14 December 2018 / Accepted: 25 March 2019 / Published online: 9 April 2019

Abstract

In this study, a model for estimating actual transpiration (T) is developed and tested for three tree species (*Olea europaea*, *Citrus sinensis*, *Pinus pinea*), growing in rainfed conditions in urban environment under Mediterranean semi-arid climate. The model, previously tested on many field crops, is based on the "big leaf" Penman-Monteith (PM) formulation of T in which canopy resistance (r_c) is modeled with respect to local climatological conditions in different plant water status. Here r_c is expressed as a function of available energy, vapor pressure deficit and aerodynamic resistance, and the trees' water status was evaluated by means of crop water stress index. On an hourly scale, the comparison with T measured by sap flow thermal dissipation technique shows good performances of the model for all investigated species under contrasting water stress conditions. At daily scale, T modeled is less accurate for all species, because of the lack of stationarity conditions in the PM approach. At seasonal scale, however, the model gives good estimation of T, with an underestimation of − 1% for *Olea* and *Pinus* and overestimation of + 8% for *Citrus* with respect to the measured T values. The proposed model needs species-specific experimental calibration, but it may have good perspective of applicability in supporting water irrigation planning in urban forestry.

1 Introduction

Transpiration of urban trees is yet a highly uncertain term of water balance of towns (Pataki et al. 2011a; Litvak et al. 2017). The uncertainty is due to the difficulties in both measurement and modeling of transpiration in urban environments, because of the large heterogeneity of vegetated surfaces. In particular, the quantification of actual transpiration rate of urban vegetation is complicated by different responses to water and energy availabilities by different cohabitant species growing in the same area (Chen et al. 2011, 2012).

Transpiration is part of latent heat flux, a component of the energy balance which can be measured, at city scale, by the eddy covariance (EC) micrometeorological method (Aubinet et al. 2012). By EC approach, latent heat has been linked to the structure of urban environment at different time scales (Loridan and Grimmond 2012). However, in heterogenic vegetated surfaces, any detail can be given by EC about the transpiration of single tree species, by preventing accurate estimation of urban and regional water budgets (e.g., Shields and Tague 2012; Vahmani and Hogue 2014b) and, then, municipality water allocation planning (Pataki et al. 2011a). For these purposes, transpiration needs to be quantified at hourly, daily, and season scales, taking into account the different behavior of the vegetated surfaces involved.

Generally, two methods are currently used to estimate the evapotranspiration (ET, plant transpiration plus surface evaporation) or transpiration (T, when evaporation, E, is neglected) of vegetated urban surfaces.

The first method is a two-step model (e.g., Spano et al. 2009; Vahmani and Hogue 2014a, b; Litvak et al. 2017), where ET is calculated as product of the landscape coefficient (K_L) and the reference evapotranspiration (ET_0) by using the following equation:

$$ET = K_L ET_0 \quad (1)$$

where K_L is a reworking of the crop coefficient K_c used for field crops, firstly introduced by Doorenbos and Kassam (1979) and updated by Allen et al. (1998) and expressed as function of (i) species-specific differences in transpiration, (ii) planting density, and (iii) micro-climatic conditions (Costello

✉ Gianfranco Rana
gianfranco.rana@crea.gov.it

[1] CREA Research Centre for Agriculture and Environment, 70125 Bari, Italy

[2] CREA Research Centre for Forestry and Wood, 52100 Arezzo, Italy

et al. 2000; Litvak et al. 2017); ET_0 is usually calculated on the base of the Penman-Monteith (PM) combination equation (Monteith 1965) applied to a reference surface, usually grass, where canopy resistance (r_c) is supposed to be constant in time and in different sites where it is applied (Katerji and Rana 2011). The value of this fixed resistance depends on the time scale considered for the calculation of ET_0. The two-step model has the advantage of using the standard weather variables collected by standard weather stations. The accuracy of the *ET* values determined by Eq. (1) depends on two factors: firstly, on the accuracy of the ET_0 determination in different geographical sites, then, on the accuracy of the K_L values.

The second approach is the one-step model (e.g., Grimmond and Oke 1991; Mitchell et al. 2008; Chen et al. 2012; Ballinas and Barradas 2015), which directly calculates the *ET* of a crop without a step through a reference surface. This model applies the PM equation where r_c is (i) specific for each species, (ii) function of climatic characteristics of the atmosphere above the urban surface inside the boundary layer, and (iii) depending on the crop water status. The parameterization of r_c is based on modeling works (Jarvis 1976; Fanjul and Barradas 1985; Grimmond and Oke 1991; Barradas et al. 2004). The one-step model requires fewer computation steps and, consequently, it is less prone to error sources than the two-step model (Rana et al. 2012).

Typically, *ET* models have been applied to urban trees: (i) in well-watered conditions (Litvak et al. 2017); (ii) using empirical methods for taking into account the plant water stress (Grimmond and Oke 1991; Barradas et al. 2004; Spano et al. 2009; Ballinas and Barradas 2015; Riikonen et al. 2016); and (iii) in conditions where there were no effects of water shortage on plants (Chen et al. 2012). Indeed, the application of *ET* models in arid and semi-arid ecosystems, where rainfed crops often experience water stress conditions, is very challenging regarding the canopy resistance estimation. In fact, it is very difficult to estimate r_c in different soil, climate, and crop water conditions. In fact, many experiments demonstrated that r_c is affected, instantaneously, by solar radiation, vapor pressure deficit, leaf water potential, soil water content (see, for example, the reviews by Rana and Katerji 1998; Katerji and Rana 2011), and hormonal messages (Davies et al. 1986; Schulze 1986). A simple method for modeling this resistance term is a preliminary condition for applying the PM model in urban environments where the optimal water condition is not assured. However, the PM model was established on hourly scale which is not the best time scale choice for applicative purposes, usually performed at daily and seasonal scales. Furthermore, the response of canopy resistance to crop water conditions can be observed on an instantaneous scale, thus leading to important fluctuations of r_c during the day (e.g., Rana et al. 1997a; Barradas et al. 2004); hence, the determination of r_c throughout the mean daily value becomes arbitrary without a suitable site-specific analysis (Katerji and Rana 2011).

This study proposes a model of transpiration, based on one-step PM approach, applied to three rainfed species (*Olea europaea* L., *Citrus sinensis* L., and *Pinus pinea* L.) growing in an old multi-species garden in the downtown city under semi-arid Mediterranean climate conditions. The objectives are (i) to establish a criterion for identifying the trees' water stress conditions, (ii) to model, at hourly scale, the canopy resistance by a deterministic approach based on the response of r_c to the climate in different trees' water conditions, (iii) to model at daily scale the actual trees' transpiration through site-specific coefficients, and (iv) to estimate the trees' water requirements at seasonal scale.

The key idea is to design a canopy resistance model in the PM equation, already successfully applied to open field crops and trees (Rana et al. 1994, 1997a, b, c, 2001, 2005), to estimate actual transpiration of rainfed urban trees.

2 Materials and methods

2.1 The site

The investigated trees are part of a multi-species garden (surface 12,780 m^2) located within the city of Bari in southern Italy on the Adriatic Sea (Fig. 1). The garden is owned by CREA-AA, and it is inside an area that comprises public and home buildings, public offices, schools, and the University Campus. The CREA-AA building hosts a research institute since more than one century, being established in 1881; the majority of trees (about 80%) was planted between the last decades of the nineteenth century and the first decades of the twentieth century.

The site is in the Mediterranean region (EEA 2016), submitted to "warm temperate with hot and dry summer" climate, following the Köppen-Geiger climate classification (Kottek et al. 2006). The mean annual temperature is 16.1 °C with a mean annual precipitation of 567 mm, calculated over the period 1995–2015. Moreover, using the aridity index defined by Holdridge et al. (1971), the climate of the region can be currently defined as dry (Ferrara et al. 2017).

The soil is classified as "Lithic Rhodoxeralf" and is characterized by clay texture, stable structure, cracked limestone subsoil, and fast drainage. The experiment was carried out in 2015 during the hottest period in the region, i.e., from 14 May to 2 August.

About 40% of the total courtyard area is occupied by trees' projected crown; one half of this surface is occupied by *Olea*, *Citrus*, and *Pinus* trees (10.9%, 1.6%, 7.5% of surface, respectively, with 38 Olea, 42 Citrus, and 12 Pinus trees) as estimated by the Google® Planimeter tool; all other surface types in the courtyard are indicated in Table 1. To estimate the projected crown area, the crown radii of trees were measured in the four cardinal directions from the trunk for each tree (e.g., Karlik and McKay 2002). The management of the garden foresees the pruning of *Citrus* trees every 5 years (last pruning on 2013), while *Olea* trees are pruned every 6–8 years (last pruning on 2011); the other trees are never pruned except for safety issues.

Fig. 1 The studied garden with the monitored trees (indicated with letters and numbers; O *Olea*, C *Citrus*, P *Pinus*)

2.2 The model of transpiration at hourly scale

The investigated area is covered by vegetation and impervious plus rooftops for about 47% and 46%, respectively (see Fig. 1, Table 1); consequently, plants' transpiration consumes much more water than evaporation from soil (Amoroso et al. 2010; Sutanto et al. 2012). Moreover, the vegetated surface is well compacted due to no tillage and no irrigation in the garden, resulting in very low evaporation rates (Nassar and Horton 1999), only limited to short periods after rain (Symes and Connellan 2013). Furthermore, since the garden is crossed by paths and asphalted roads, after rain, the water rapidly runoff along these preferential ways, by preventing effective infiltration into the soil (Fini et al. 2017) and limiting surficial soil evaporation.

Actual crop transpiration was estimated by PM type model, which is considered appropriate also for urban inhomogeneous vegetated surfaces (Grimmond and Oke 1991; Ballinas and Barradas 2015, among others). In this model, which is theoretically applicable when the thermodynamic conditions are stationary, i.e., on hourly time scale, the latent heat flux due to transpiration, λT_c (W m^{-2}), of each studied species is written as follows:

$$\lambda T_c = \frac{\Delta Q + \rho c_p D / r_a}{\Delta + \gamma\left(1 + \frac{r_c}{r_a}\right)} \quad (2)$$

Δ is the slope of the saturation pressure deficit versus temperature function in kPa °C^{-1}; Q is the available energy in W m^{-2}; ρ is the air density in kg m^{-3}; c_p is the specific heat of moist air in J kg^{-1} °C^{-1}; D is the vapor pressure deficit in kPa; γ is the psychrometric constant in kPa °C^{-1}; r_a is the aerodynamic resistance in s m^{-1}; r_c is the bulk canopy resistance in s m^{-1}; and λ is the latent heat of evaporation in J kg^{-1}.

r_a was calculated between the top of the trees and a reference point (z) where the measurements of weather variables were carried out, according to Perrier (1975) as follows:

Table 1 Fraction and characteristics of each surface type in the study site. Albedo values from Brutsaert (1982); heat capacity values from Brutsaert (1982) and Offerle et al. (2005); thickness values are estimated following Offerle et al. (2005). The a_i coefficient ($i = 1, 2, 3$) for the sensible heat storage model (Roberts et al. 2006) are reported with relative references

Surface type		Fraction (%)	Albedo	Heat capacity (MJ m^{-3} °C^{-1})	Thickness Δx_i (m)	a_1	a_2	a_3 (W m^{-2})	References
Greenspace	Grass	7	0.21	3.31	0.8	0.32	0.54	−27.4	Doll et al. (1985)
	Bare soil	7	0.05	3.31	0.8	0.38	0.56	−24.3	Novak (1981)
	Mixed forest and shrubs	40	0.18	7.61	0.8	0.11	0.11	−12.3	McCaughey (1985)
Rooftops		19	0.25	5.25	0.12	0.82	0.34	−55.7	Yoshida et al. (1990–1991)
Impervious	Concrete	14	0.25	2.07	0.12	0.85	0.32	−28.5	Asaeda and Ca (1993)
	Asphalt	13	0.12	2.61	0.03	0.82	0.68	−20.1	Roberts et al. (2006)

$$r_a(z) = \frac{ln[(z-d)/(h_t-d)]}{ku^*} \quad (3)$$

where d (m) is the zero-plane displacement and is estimated by $d = 0.67h_t$; h_t (m) is the mean height of the trees of the same species; k is the von Kármán constant (0.40); and u^* is the friction velocity (m s^{-1}). The wind speed (m s^{-1}) measured at the reference point z above the canopy was expressed as follows (e.g., Arya 2001):

$$u(z) = \frac{u^*}{k} ln \frac{z-d}{z_0} \quad (4)$$

where z_0 (m) is the roughness length estimated by $z_0 = 0.1h_t$. z_0 is a measure of the aerodynamic surface heterogeneity, in this case, vegetation (Ballinas and Barradas 2015). Therefore, the final formula for r_a was written as follows:

$$r_a(z) = \frac{ln[(z-d)/z_0]ln[(z-d)/(h_t-d)]}{k^2 u(z)} \quad (5)$$

The use of this relationship for the aerodynamic resistance introduces two simplifying assumptions on the homogeneity of the transpirative layer which needs to be evaluated: (i) r_a was assumed to be the same for the whole tree canopy; (ii) r_a was assumed to be the same for all trees of same species. The first simplification implies that the source/sink of boundary layer fluxes was at the same height, with no difference among leaves at different positions in the tree canopy. This assumption is supported by the study of Daudet et al. (1999), who found that wind velocity profile and direction weakly influenced the transpiration rate along the tree canopy; thus, the error can be considered negligible. The second assumption on r_a implies that the calculation of d and z_0 in Eq. (5) was made at the same height h_t of all trees of the same species. A sensitivity analysis on r_a (data not shown) with respect to these parameters showed that a variation of 50% of their values determined an error in the range 10–15% when the wind speed varied between 1 and 5 m s^{-1}.

2.2.1 The canopy resistance parametrization

The PM formula is the combination of two terms: (i) the radiative term and (ii) the aerodynamic term. To clearly separate these two terms, Eq. (2) can be written under the following form:

$$\lambda T_c = \frac{\Delta}{\Delta+\gamma} Q \frac{1 + \frac{\rho c_p D}{\Delta Q r_a}}{1 + \frac{\gamma}{\Delta+\gamma}\frac{r_c}{r_a}} \quad (6)$$

From the above relation, it can be argued that there are only two cases in which λT_c is equal to the radiation term (i.e., λT_c independent of the aerodynamic term): (i) when $r_a >> 0$, i.e., the surface is very smooth which is unusual in urban situation (Grimmond and Oke 1999) and/or the wind speed is very low; (ii) when r_c takes the particular value:

$$r_c = \frac{\Delta+\gamma}{\Delta\gamma}\frac{\rho c_p D}{Q} = r^* \quad (7)$$

This last variable is linked to the "isothermal resistance" introduced for the first time by Monteith (1965). It has also been called "critical resistance" (Daudet and Perrier 1968) because it represents a threshold between two conditions: (i) $r_c < r^*$ and T_c increases with wind speed; (ii) $r_c > r^*$ and T_c decreases with wind speed (Rana et al. 1994).

If we substitute Eq. (7) into Eq. (6), the PM formula can be written in a more symmetric form where the mentioned resistances r^*, r_a, and r_c clearly appear in the aerodynamic term as:

$$\lambda T_c = \frac{\Delta}{\Delta+\gamma} Q \frac{1 + [\gamma/(\Delta+y)](r^*/r_a)}{1 + [\gamma/(\Delta+\gamma)](r_c/r_a)} \quad (8)$$

The first term is the equilibrium transpiration (Jarvis 1976; Jarvis and McNaughton 1985), and the second fraction is a dimensionless quantity which provides the aerodynamic weighting on the equilibrium transpiration (McNaughton 1976) and can be seen as a crop-climatological coefficient: it modulates the part of the available energy transformed by the soil-canopy-atmosphere system during transpiration. It was experimentally demonstrated (e.g., Perrier et al. 1980; Rana et al. 1997b; Shi et al. 2008; Rana et al. 2012) that r_c/r_a was a function of r^*/r_a and this relationship depended on phenological stage and crop water status. In fact, following the fluid mechanics data analysis approach, a relationship between r_c/r_a and r^*/r_a can be argued from a dimensional analysis based on the Buckingham theorem (e.g., Kreith 1973) as:

$$\frac{r_c}{r_a} = f\left(\frac{r^*}{r_a}\right) \quad (9)$$

Katerji and Perrier (1983) firstly proposed a linear relation for f in Eq. (9); in the next, many authors experimentally demonstrated the validity of such relationship and the accuracy in the estimation of actual evapotranspiration of different crops (see the synthesis in Katerji and Rana 2013).

The evaluation of the presented model were carried out through two steps: (i) the calibration, i.e., the search for the experimental function "f" linking the ratios r_c/r_a and r^*/r_a (see Eq. 9), and (ii) the validation with the comparison between calculated and measured actual transpiration values. In the present case (see

Section 3.2), the best fitting function was found to be logarithmic for all species as:

$$\frac{r_c}{r_a} = a\, ln\left(\frac{r^*}{r_a}\right) + b \tag{10}$$

2.2.2 The available energy *Q* and the measurement of weather variables

The energy available to the trees (Q) can be expressed, following a common nomenclature for urban energy balances (Grimmond and Oke 1991; Christen and Vogt 2004), as:

$$Q = Q^* + Q_F + Q_A + Q_S \tag{11}$$

where Q^* is the net all-wave radiation (W m^{-2}), Q_F is the anthropogenic heat release (W m^{-2}), Q_A is the net heat advection (W m^{-2}), and Q_S is the sensible heat storage (W m^{-2}). In this study, (i) Q^* was measured by net radiometers; (ii) Q_F, including all additional energy inputs produced by human activities, such as the energy released by combustion of fuels, electric heating, air conditioning, and traffic, can be considered negligible since the garden is in a residential area with many public buildings and the traffic is strongly seasonal and limited to their opening/closing time (Loridan and Grimmond 2012); (iii) Q_A can be neglected because the experimental site is on the coast of Adriatic Sea, beneficiating of the sea breeze regime (Christen and Vogt 2004; Lemonsu et al. 2004; Loridan and Grimmond 2012); and (iv) Q_S was estimated according to the "objective hysteresis model" of Grimmond et al. (1991) as upgraded by Roberts et al. (2006):

$$Q_S = \sum_{k=1}^{n} (f_k a_{1k}) Q^* + \sum_{k=1}^{n} \left(f_j a_{2k}\right) \frac{\partial Q^*}{\partial t} + \sum_{k=1}^{n} f_k a_{3k} \tag{12a}$$

$$\frac{\partial Q^*}{\partial t} \approx 0.5\left(Q^*_{t-1} - Q^*_{t+1}\right) \tag{12b}$$

where f_k indicates the fractions of space occupied by each surface type. Namely, 6 types of surface were identified: grass, bare soil, mixed forest and shrubs, rooftops, impervious concrete, and asphalt. The coefficients a_1, a_2, and a_3 were derived from independent studies on urban surface types and their values are reported in Table 1. t is the time interval (60 min, following the time interval of measurements).

A meteorological station (Weather transmitter WXT520, Vaisala, Helsinki, Finland) was set up on the CREA-AA building; it measured precipitation, temperature, and relative humidity of air, wind, speed, and direction. Global radiation was measured by a pyranometer (CMP3, Kipp & Zonen, Delft, The Netherlands). Net radiation (Q^*, W m^{-2}) was measured by two net radiometers (Q^*6, REBS, USA). All measurements were taken by data loggers (CR800, CR10X, Campbell Scientific, Utah, USA) every 10 s, and the average values recorded every 60 min. The sensors of the meteorological station were installed on a 1.5-m-high mast mounted on a little tower (2 m height) on the roof of the building at 12 m from ground level. Thus, the reference level of all meteorological variables was set at $z = 15.5$ m from the ground.

2.3 The model of transpiration at daily and seasonal scales

To calculate daily T_c, two methods could be used.

(1) T_c is estimated as the sum of hourly data so that:

$$T_{cd} = \sum_{h=1}^{24} T_{c,h} \tag{13}$$

with $T_{c,h}$ is the hourly values expressed by Eq. (2). This method, theoretically the most correct, is not practical since the parameters measured on an hourly scale are needed.

(2) The second method is based on a simplification of the relationship (8), so it can be written as:

$$T_{cd} = K_d \frac{1}{\lambda}\left(\frac{\Delta}{\Delta+\gamma}\right)_d Q_d \tag{14}$$

where

$$K_d = \frac{1 + [\gamma/(\Delta + y)](r^*/r_a)_d}{1 + [\gamma/(\Delta+\gamma)](r_c/r_a)_d} \tag{15}$$

The subscript d indicates the daytime average.

It was experimentally demonstrated (Katerji and Perrier 1983; Katerji et al. 1990; Rana et al. 1997a) that, for field crops in good water conditions, the K_d coefficient varies little with the r^*/r_a ratio and, in a first approximation, could be considered constant, while K_d varies considerably with the crop water status (Itier et al. 1992) and it seems that this last variation is a plant species characteristic (Rana et al. 1997b, c).

In the present study, in analogy to the hourly time scale, the coefficient K_d was calculated as function of the ratio $(r^*/r_a)_d$, i.e., the daily average of r^*/r_a; the best fitting function was found to be logarithmic for all species as (see Section 3.2):

$$K_d = A\, ln\left(\frac{r^*}{r_a}\right)_d + B \tag{16}$$

Transpiration at season scale was calculated by cumulating daily values.

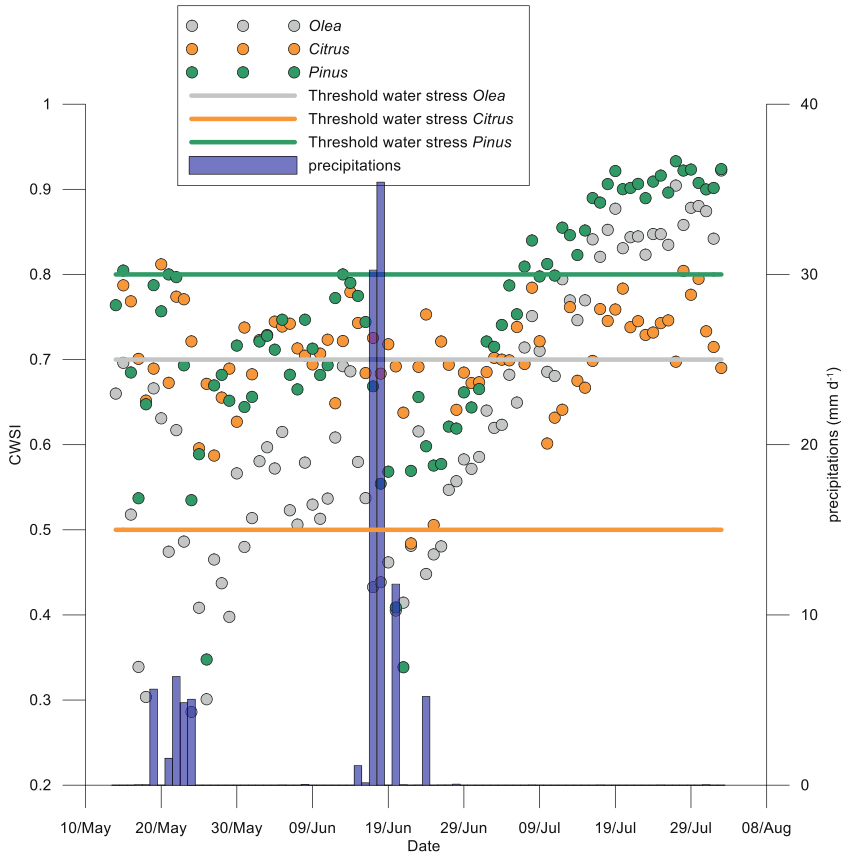

Fig. 2 CWSI patterns at daily scale for all investigated trees species; precipitations are also shown

2.4 The trees' water conditions

The leaf water potential (LWP in MPa) measured with a pressure chamber has been demonstrated to be the most accurate method for determining the physiological water stress of plants (for trees, see, for example, the review by Wullschleger et al. 1998). For field crops, Rana et al. (1997a, b) demonstrated that the coefficient K_d can be modeled in function of predawn leaf water potential (PLWP), a good indicator of crop water stress (Katerji and Hallaire 1984; Tardieu et al. 1990). By common agreement, soil water shortage has not a significant influence on gas exchanges and, consequently, on crop growth if PLWP values are above a critical species-specific threshold. For applicative purpose, the measurement of PLWP cannot be routinely carried out, while a good alternative can be to consider the available soil water (AW), defined as the amount of water in the soil, normalized by the total water availability (between field capacity and wilting point). However, the accurate monitoring of soil moisture in urban gardens and parks is quite complicated due to the inhomogeneity of the areas since, as abovementioned, besides vegetation, different types of surfaces (bare soil, concrete, asphalt) are present (Nielsen et al. 2007).

Therefore, methods to detect water stress based on the surface temperature of the crop, like the Crop Water Stress Index (*CWSI*), can be a good compromise between accuracy and feasibility (Stanghellini and De Lorenzi 1994). In this study, *CWSI* is calculated in function of actual (T_{act}) and potential (T_p) transpiration (e.g., Jackson et al. 1981; Stanghellini and De Lorenzi 1994):

$$CWSI = 1 - \frac{T_{act}}{T_p} \tag{17}$$

where T_p is calculated by the PM Eq. (2) with canopy resistance assumed equal to the minimum resistance (r_{min}). In this case, we used the following values of r_{min}: 200 s m^{-1} for *Olea europaea*, 160 s m^{-1} for *Citrus sinensis* (Körner et al. 1979), and 170 s m^{-1} for *Pinus pinea* (Kelliher et al. 1995).

The daily *CWSI* has been calculated adding up hourly transpiration values, considering only daytime ones.

2.4.1 The measured transpiration

The actual tree transpiration is needed to determine the *CWSI* values and to validate the proposed applicative transpiration model.

T_{act} was determined by sap flow heat dissipation method (HDM; Granier 1985, 1987). By HDM at first, the sap flow density J_{s0} (g_{H2O} m^{-2} s^{-1}) is determined in the outermost sapwood area, then J_{s0} must be extrapolated to all active water-conducting xylems of the sapwood area (SWA in m^2). SWA was determined by measuring sapwood depth on a core

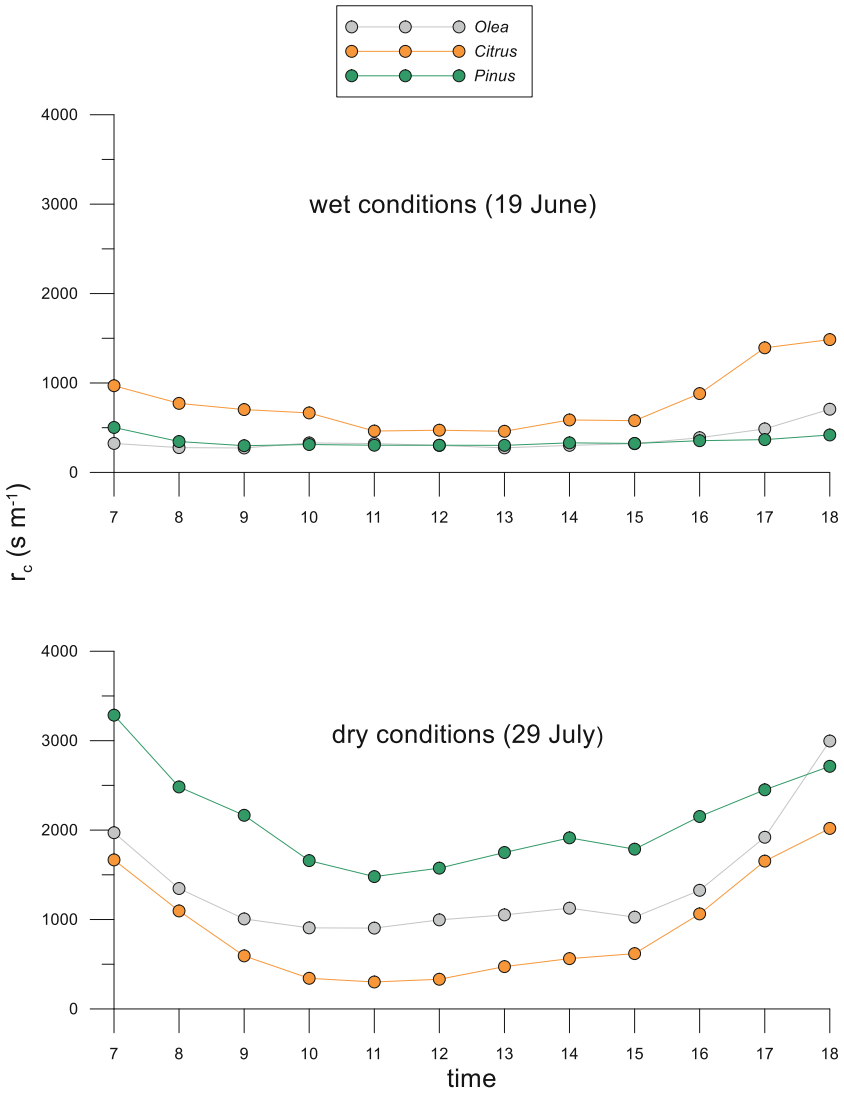

Fig. 3 Canopy resistance (r_c) patterns at hourly scale during two sample days

collected with a 5-mm-diameter increment borer at breast height in the north side of monitored trees.

The monitored trees were chosen by combining two procedures: (1) the quantile upscaling method (Čermák et al. 2004) and (2) the analysis of the frequency distribution of stem diameters (Rana et al. 2005): 4 *Olea*, 4 *Citrus*, and 3 *Pinus* trees were monitored as shown in Fig. 1.

To avoid direct solar heating, the sap flow probes (20 mm, SFS2 Type M, UP, Steinfurt, Germany) were installed at breast height in the north side of each tree (Lindén et al. 2016), covered by a reflecting radiation screen, which also protects from rain. J_{s0} was continuously monitored every 10 s, and 10-min averages were stored by data loggers (three CR10X, Campbell Scientific, UT, USA). Hourly values were obtained by averaging the 10-min data.

To account for radial trends in sap flux density, according to Pataki et al. (2011b) and Litvak et al. (2012), the sapwood depth was divided in a set of 2-cm increments and generalized Gaussian functions were applied to estimate the sap flux density in each increment. We used two different functions for angiosperms and gymnosperms (Pataki et al. 2011b; Litvak et al. 2012) to calculate J_{si}, i.e., the sap flux density in each increment i:

$$\text{Angiosperms}: J_{si} = 1.033 J_{s0} \exp\left(-0.5\left(\frac{x-0.09963}{0.4263}\right)^2\right) \quad (18)$$

$$\text{Gymnosperms}: J_{si} = 1.257 J_{s0} \exp\left(-0.5\left(\frac{x+0.3724}{0.662}\right)^2\right) \quad (19)$$

where x is the normalized depth of each sapwood increment ($0 \le x < 1$) and J_{s0} is calculated using the standard relationship in HDM:

$$J_{s0} = a\left(\frac{\Delta T_{\max} - \Delta T}{\Delta T}\right)^b \quad (20)$$

where ΔT (*C) is the temperature difference between the heated upper probe and the lower reference one and $\Delta T_{\max}$

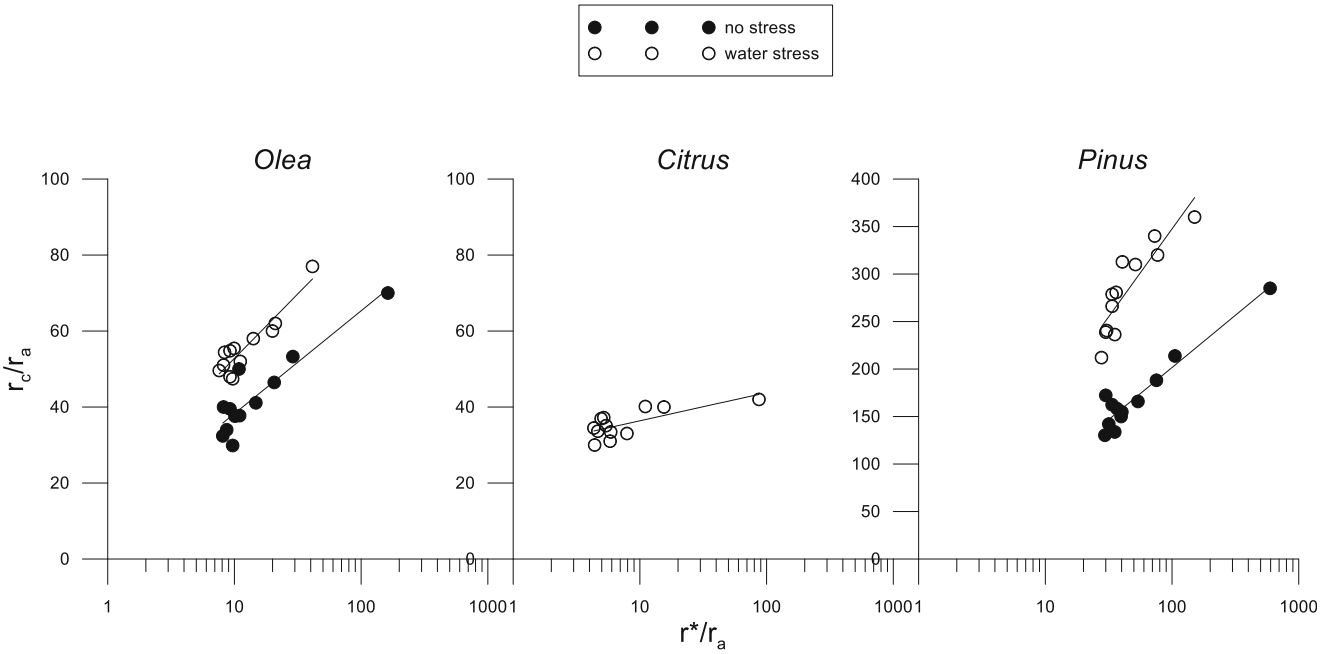

Fig. 4 Calibration of the presented model at hourly scale (see text for details)

(°C) is the maximum difference in temperature during night.

The whole tree transpiration of each sample was determined as:

$$T_{\text{act}} = \sum_{i=0}^{m} J_{si} SWA_i \tag{21}$$

where T_{act} is in g s^{-1}, m is the number of 2-cm increments in sapwood depth, J_{si} is the sap flux density (g m^{-2} s^{-1}), and SWA_i is the sap wood area at depth i. The tree's transpiration per day (kg day^{-1}) was calculated as the sum of hourly values during the daytime (global radiation, $R_g > 20$ W m^{-2}). For each species, the considered transpiration is the mean of T_{act} of all sampled trees. The transpiration per unit canopy area was calculated in kg m^{-2} (mm of transpired water) as the value of T_{act} of the species divided by the mean projected canopy area.

2.5 Statistical analysis

Following Legates and McCabe (1999), the analysis of performances (Microsoft Excel® 32 bit) of the described model at hourly and daily scale included linear regression analysis, root mean square error (RMSE), mean absolute error (MAE), model efficiency (EF, range $-\infty$ to + 1, optimum value 1), and index of agreement (d, range 0 to + 1, optimum value 1).

2.6 Sensitivity analysis of the model

A sensitivity analysis of the model with respect to the calibration parameters, p_i (i.e., the coefficients "a" and "b" in the logarithmic functions of Eq. 10), is carried out to investigate on how an error on these parameters is propagated to the estimation of tree transpiration.

Following Rana and Katerji (1998), the sensitivity analysis was carried out by calculating the non-dimensional relative sensitivity coefficients:

$$S_{p_i} = \frac{\partial \lambda T_c}{\partial p_i} \frac{p_i}{\lambda T_c} \tag{22}$$

which represent that fraction of the change in p_i that is transmitted to change λT_c. Thus, at hourly scale, the sensitivity coefficients for a and b are expressed by the following expressions:

Table 2 Calibration of the presented model at hourly scale

	Olea	*Citrus* (water stress)	*Pinus*
No stress	$r_c/r_a = 11.7 \ln(r^*/r_a) + 11.2$ $r^2 = 0.83$	$r_c/r_a = 4.11 \ln(r^*/r_a) + 22.0$	$r_c/r_a = 46.2 \ln(r^*/r_a) - 12.4$ $r^2 = 0.91$
Water stress	$r_c/r_a = 14.7 \ln(r^*/r_a) + 18.6$ $r^2 = 0.86$	$r^2 = 0.67$	$r_c/r_a = 80.3 \ln(r^*/r_a) - 22.4$ $r^2 = 0.71$

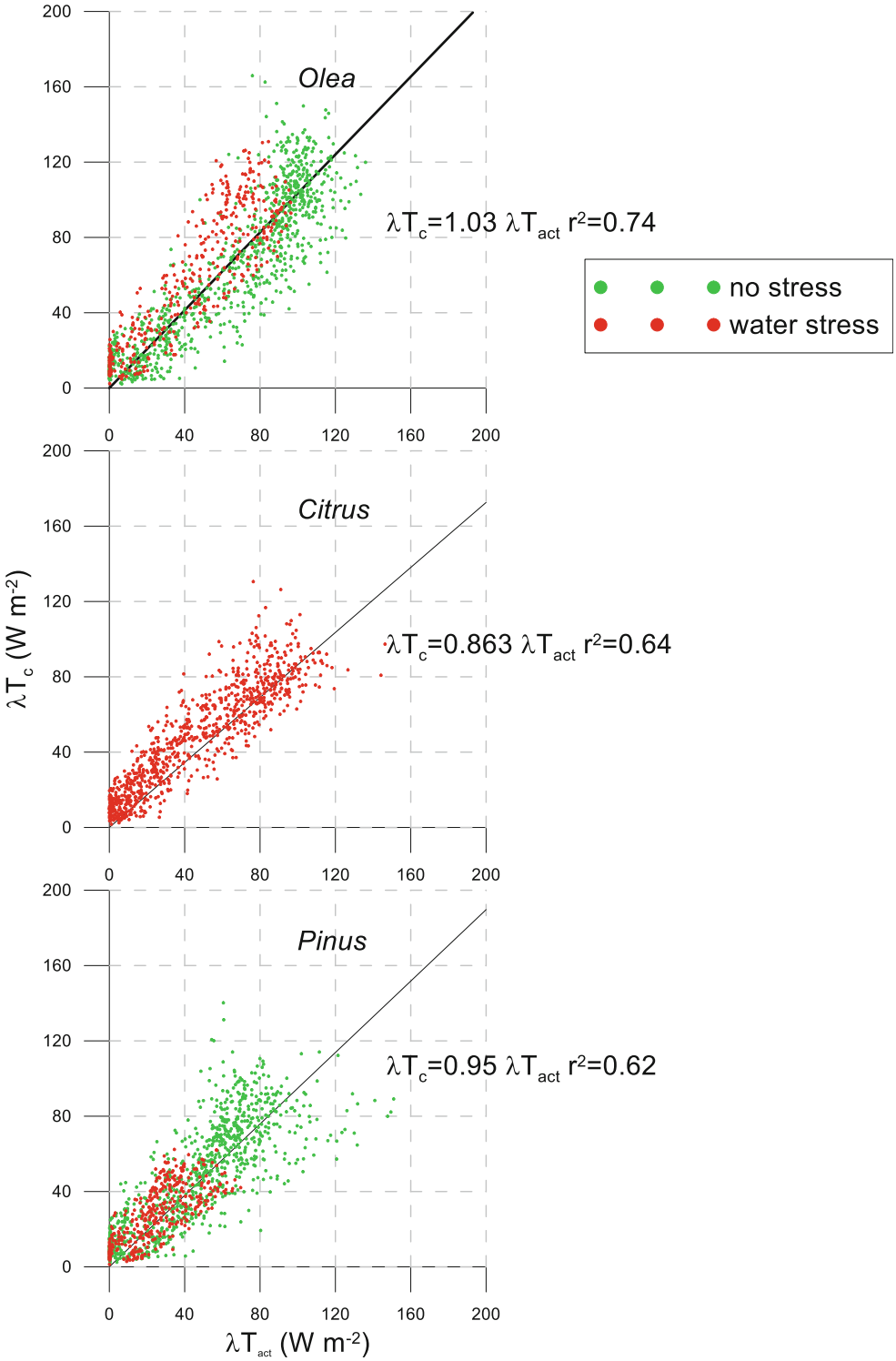

Fig. 5 Comparison between calculated (λT_c) and measured transpiration (λT_{act}) at hourly scale; trees' water conditions are also indicated for the species under investigation

$$S_a = -a\frac{(1-C)\ln\left(\frac{r^*}{r_a}\right)}{1+(1-C)\left[a\ln\left(\frac{r^*}{r_a}\right)+b\right]} \quad (23)$$

$$C = \frac{\Delta}{\Delta+\gamma} \quad (24)$$

$$S_b = -b\frac{1-C}{1+(1-C)\left[a\ln\left(\frac{r^*}{r_a}\right)+b\right]} \quad (25)$$

where

Table 3 Statistics of the presented model at hourly and daily scales

Time scale	*Olea*				*Citrus*				*Pinus*			
	RMSE	MAE	EF	*d*	RMSE	MAE	EF	*d*	RMSE	MAE	EF	*d*
Hourly	20 W m^{-2}	15 W m^{-2}	0.71	0.93	25 W m^{-2}	15 W m^{-2}	0.63	0.87	17 W m^{-2}	15 W m^{-2}	0.66	0.90
Daily	0.34 mm day^{-1}	0.56 mm day^{-1}	− 0.38	0.88	0.34 mm day^{-1}	0.51 mm day^{-1}	− 0.67	0.85	0.32 mm day^{-1}	0.48 mm day^{-1}	0.23	0.90

Negative coefficients indicate that a reduction in λT_c results from an increasing of p_i. By these coefficients, it is possible to evaluate the effect, on λT_c, due to error on the determination of the input parameters. In fact, following the definition of relative error in a function due to relative errors in the input data, it is possible to write the relative error expression for transpiration as:

$$\varepsilon_{\lambda T_c} = |S_a|\varepsilon_a + |S_b|\varepsilon_b \tag{26}$$

with $\varepsilon_{\lambda Tc}$, ε_a, and ε_b relative error on λT_c, a, and b, respectively.

3 Results and discussion

3.1 The weather and the trees' water conditions by *CWSI*

The daily patterns of R_g (between 7.8 and 31.0 MJ m^{-2} day^{-1}), T_a (between 10.4 and 31.2 °C), and D (between 0.6 and 3.1 kPa) were typical of the region in the investigated season (data not shown). The precipitation amounts during the study period were high in the second half of May and, mostly, in mid-June (79 mm from 15 to 20 June, Fig. 2), which is usually dry in this area.

The *CWSI* showed, at hourly scale, very variable and spread values (data not shown) for all species, since it is function of input variables rapidly and instantaneously changing (Stanghellini and De Lorenzi 1994; Rana and Katerji 1998). However, at daily scale, the *CWSI* trends (Fig. 2) appeared clearer and able to suitably detect the water status of the investigated trees.

Berni et al. (2009) demonstrated that for *Olea* growing under Mediterranean climate, significant relationships can be found among the leaf stem potential, the canopy conductance, and the *CWSI*. Ben-Gal et al. (2009) showed that when an olive orchard in arid environment was irrigated with an amount of water between 100 and 50% of potential ET, the daily *CWSI* values were between 0.2 and 0.4, while when the water supplied was only 25% of potential ET, then the *CWSI* was around 0.7. Agam et al. (2013) showed that the maximum value of *CWSI* (calculated by the standard approach as in the present case) achieved by irrigated olive trees was again around 0.7. Therefore, in this study, we fixed at 0.7 the value of *CWSI* above that the *Olea* trees were in water stress (see Fig. 2).

Gonzalez-Dugo et al. (2013) in *Citrus* orchard found that any clear relationship can be envisaged between LWP and *CWSI* and that the *CWSI* values are always below 0.6–0.7 even if the irrigation was stopped for inducing water stress. Similar results were found by Waldo and Schumann (2009) and Ballester et al. (2013), and these last authors showed a maximum value of *CWSI* around 0.5 also when the *Citrus* trees were induced to water stress. Gonzalez-Dugo et al. (2014) found that when

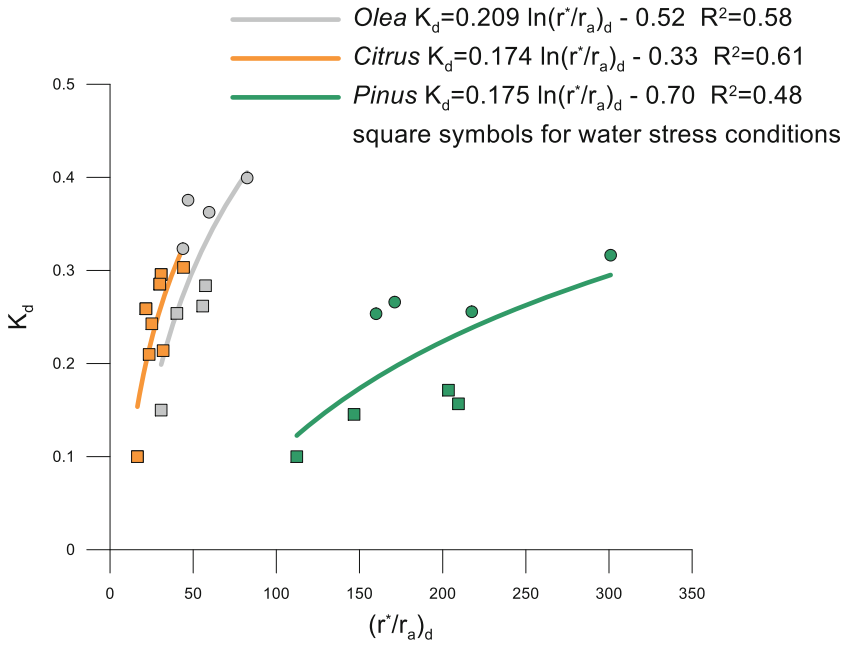

Fig. 6 Calibration of the model at daily scale (see text for details)

Citrus CWSI values attained 0.85, the crop was under severe water stress and when *CWSI* was close to 0, it was in optimal water conditions. In this case, *Citrus* trees had *CWSI* values almost always between 0.6 and 0.8 (see Fig. 2) without any significant trend. Furthermore, all studied *Citrus* trees were affected by a typical disease of this species, *Dialeurodes citri* (Homoptera: Aleyrodidae), which causes damage to crop directly through suck the sap and reducing plant vitality as well as the excretion of honeydew colonized by sooty mold fungi that reduce gas exchanges, which means photosynthesis, respiration, and transpiration (Rapisarda and Cocuzza 2017; Argov et al. 1999). Therefore, it was supposed that *Citrus* were under water stress conditions all time during this study.

For *Pinus* trees and in general for conifers, the measurement of water conditions through the *CWSI* was very rare. Seidel et al. (2016) found that the maximum *CWSI* value achieved by irrigated scots pine trees was 0.8, which was considered as the threshold value between stress and no-stress condition in this case study (see Fig. 2).

Hourly values of r_c during daytime (i.e., between 7:00 and 18:00), obtained by inverting Eq. (2) with T_c and all inputs measured, are shown in Fig. 3 for three species under investigation. Two days is reported as example: 19 June (wet), after 2 days of huge rain (76 mm in total), and 29 July, 34 days after this huge precipitation (dry). On 19 June, the daily values of *CWSI* were 0.46, 0.74, and 0.57 for *Olea*, *Citrus*, and *Pinus*, respectively, hence below the thresholds previously established for the water stress conditions for Olea and *Pinus*, while above water stress threshold for *Citrus*: *Citrus* trees' seems did not react to the huge rain in terms of transpiration due to the effect of their pest. On 29 July, the values of *CWSI* were 0.88, 0.70, and 0.92 for *Olea*, *Citrus*, and *Pinus*, respectively, hence above the water stress threshold values for all species. Under well-watered conditions during wet day, daytime r_c were in the range 274–706 and 299–503 s m^{-1}, with means of 359, and 347 s m^{-1} for *Olea* and *Pinus* respectively; these values are greater than those published by other authors for *Olea* (Berni et al. 2009) under good water conditions, while the values of r_c found for *Pinus* are in line with those found in similar environments (Hoshika et al. 2017).

During dry days, under water stress r_c was in the range 904–2995 and 1480–3286 s m^{-1} with means of 1382, and 2118 s m^{-1} for *Olea* and *Pinus* respectively, in this case, a comparison with other studies is very difficult because of the large variability in the relationships between drought conditions and trees' water status.

For *Citrus* trees, r_c ranged between 460 and 1485 s m^{-1} on 19 June, and between 302 and 2018 s m^{-1} on 29 July, and the mean values during wet and dry days were very similar (786 and 893 s m^{-1}, respectively). These high values confirm that these trees were under water stress conditions, with a typical pattern of r_c for stressed tree species (see *Olea* and *Pinus* behavior) with closure of stoma during hours of the day with decreasing values of solar radiation (Ballester et al. 2013; Gonzalez-Dugo et al. 2014).

Based on these considerations, it was supposed that *Olea* and *Pinus* trees were in well-watered conditions from the beginning of the experiments until 8 July, then they were under water stress; *Citrus* trees were under water stress conditions during the whole experimental period.

3.2 The model at hourly scale

In Fig. 4, the experimental relationships between r_c/r_a and r^*/r_a were shown for the three species under investigation in the different water conditions. Each point represented the mean of all

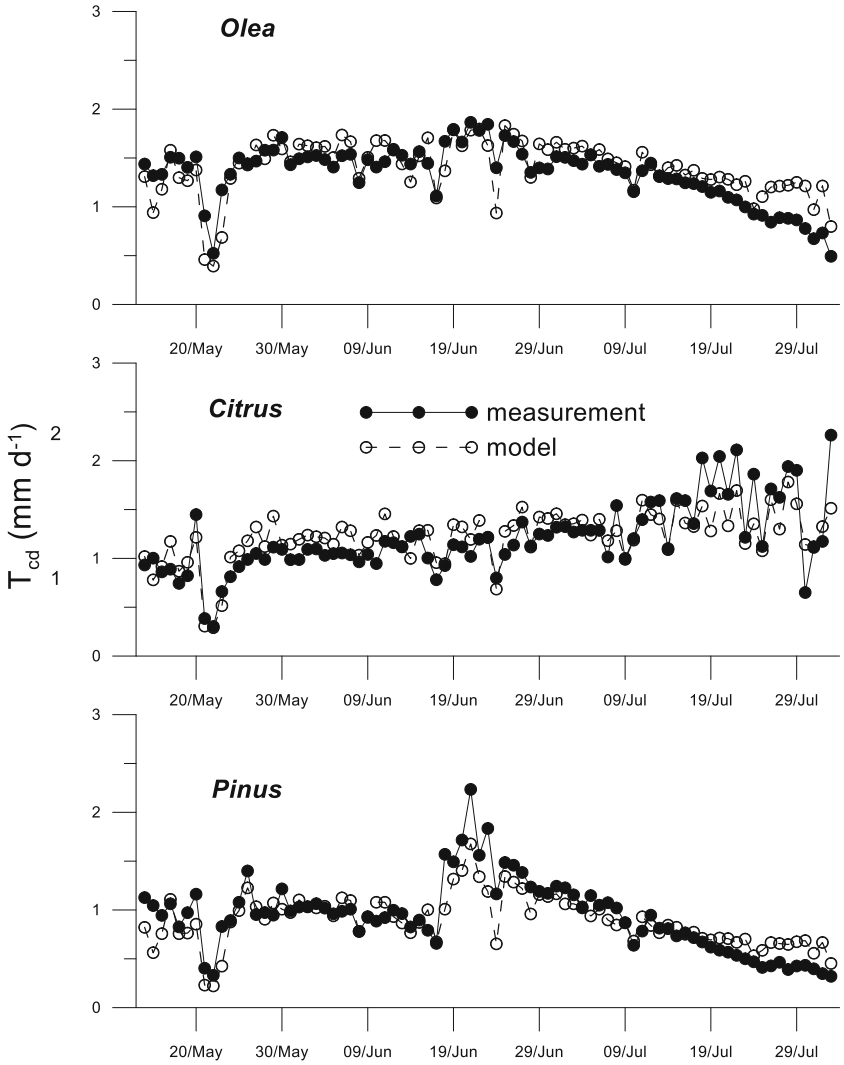

Fig. 7 Patterns of calculated and measured transpiration (T_c) at daily scale for the species under investigation during the experimental period

available hourly values during daytime (12 values from 7:00 to 18:00) in the 4 days 14–17 May (at the beginning of the experimental period in wet soil conditions) and in the 4 days 9–12 July (at the beginning of the period when also *Olea* and *Pinus* trees were under water stress conditions). The number of days for the calibration was suggested by Rana et al. (1997a, b). The logarithmic best fitting relationship between r_c/r_a and r^*/r_a are shown in Table 2: the dependence of r_c/r_a ratio on r^*/r_a was very clear for any water stress condition and for each species and quite robust (high values of determination coefficient r^2). The values of slopes of the logarithmic relationships were higher when the trees were under water stress, having higher values of r_c than the well-watered conditions for the same value of r_a at given weather conditions as expressed by r^*.

The comparison between calculated (λT_c) and measured (λT_{act}) hourly transpiration is shown in Fig. 5 for all species under investigation, excluding calibration days. Water stress and no-stress conditions are also indicated, but the regression has been made without considering water conditions, obtaining good correlation for all species. In the statistical comparison between measured and calculated values, the *t* test indicated that, in all cases, the intercept was significantly not different from zero at the 95% significance level; therefore, the analysis was done forcing the linear regression model through zero. Considering the whole experimental period, the cumulated values of estimated transpiration by the presented model indicated overestimation of 8% and 4% for *Olea* and *Pinus*, respectively, and underestimation of − 4% for *Citrus* with respect to the measured cumulated values. Other statistical indicators are shown in Table 3 indicating that the model had pretty good performances at hourly scale, with low values of the errors (RMSE and MAE), acceptable values of EF and high values of *d*.

3.3 The model at daily and seasonal scales

To calibrate the relationship between K_d and $(r^*/r_a)_d$ (Fig. 6), we used the daily values of the same days used to calibrate the hourly model (i.e., 14–17 May and 9–12 July). Like in Fig. 5, water stress and no-stress conditions are also indicated using different symbols, but the logarithmic relationships are obtained considering all data together: the parametrization is quite robust with high values of determination coefficients also at daily scale. For *Olea* and *Pinus*, the values of K_d were generally lower in water stress conditions than in well-watered conditions. The coefficient K_d calculated by these logarithmic functions was used to calculate the actual transpiration (Eq. 14) at daily scale.

A comparison between daily measured and calculated T_c is shown in Fig. 7 for the three species under investigation. For *Olea* and *Pinus*, T_c ranged between low values before precipitations and high values afterwards, while *Citrus* seems to increase its transpiration during dry periods (after 8 July). During rainy days, transpiration decreased and the model reproduced these events.

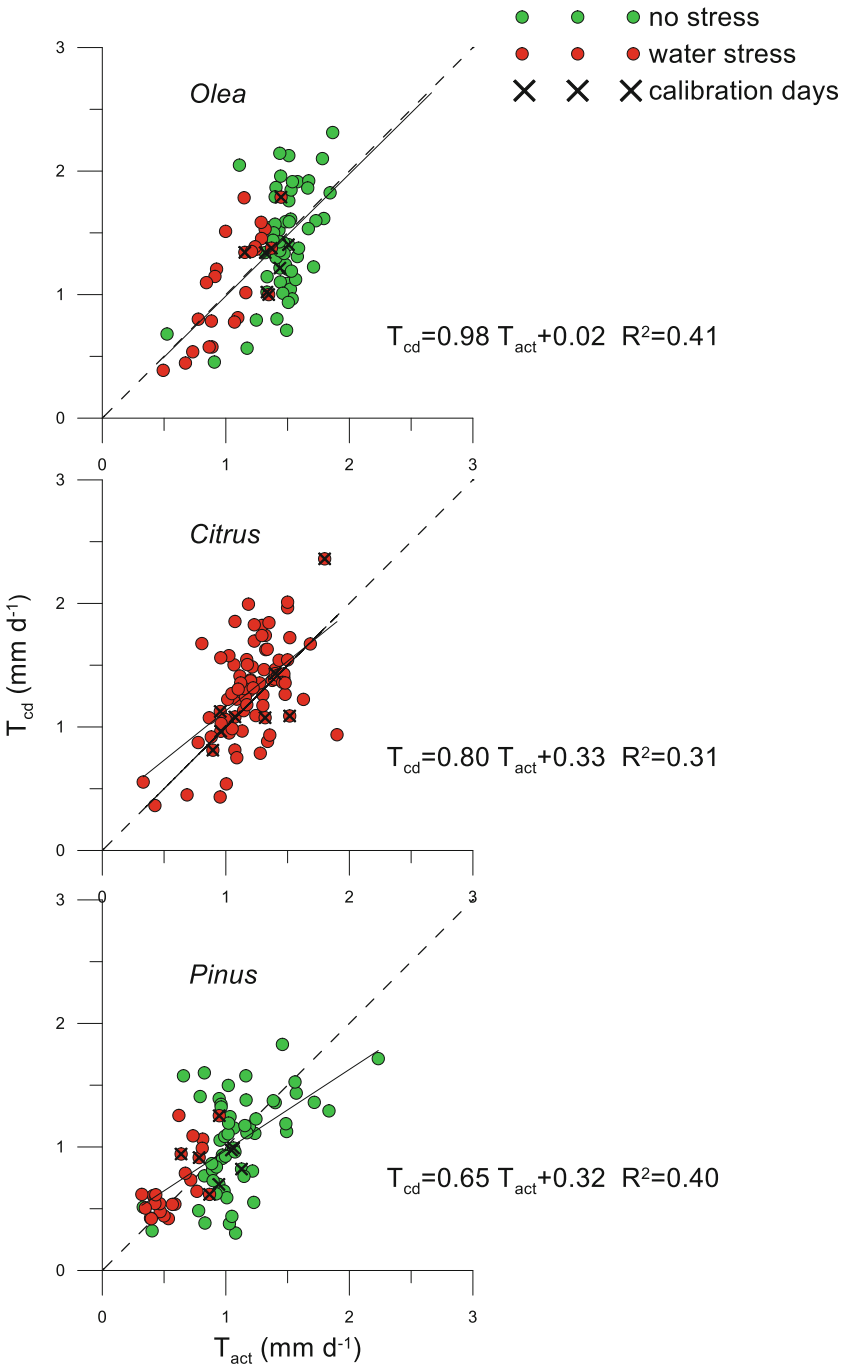

Fig. 8 Comparison between calculated (T_{cd}) and measured transpiration (T_{act}) at daily scale; trees' water conditions are also indicated for the species under investigation

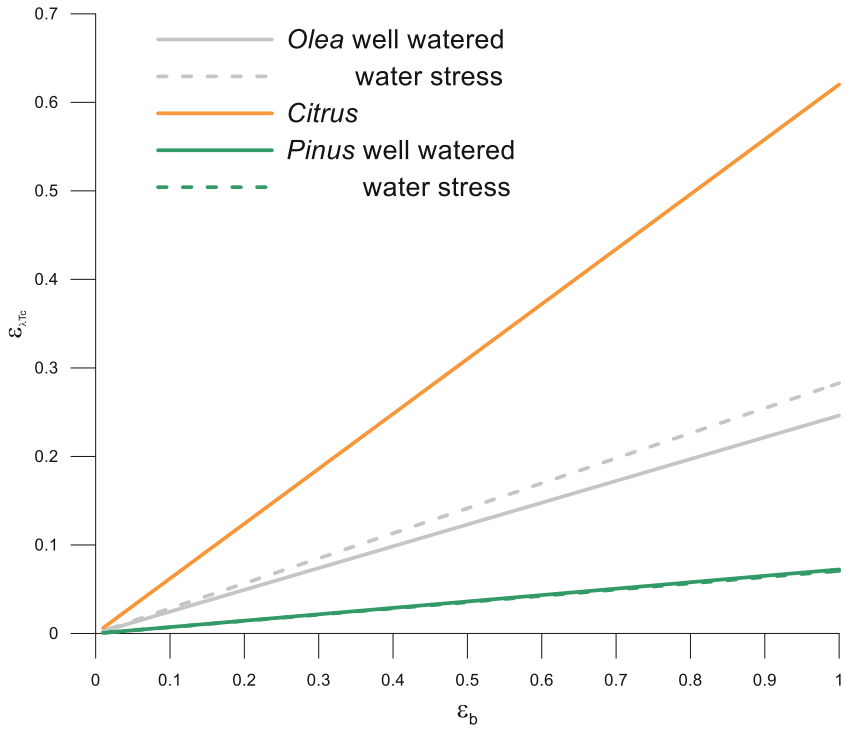

Fig. 9 The relative error on calculated transpiration due to error in the input parameter b (see Eq. (10)) for both stress and no-stress conditions

The linear regression statistical analysis between the modeled and measured T_c is shown in Fig. 8 and both well-watered and stress conditions are also indicated, but the regression is done considering all together and excluding the calibration days. In this case, the comparison showed that the daily model is much less accurate (low R^2) than the model at hourly scale. The other statistical indicators (see Table 3) indicated that at daily scale, the model presented worst performances than at the hourly scale, with pretty high values of *RMSE* and *MAE* and low values of *EF*, even if the index of agreement *d* had pretty high values. The loss of accuracy of the daily model with respect to the hourly one was due to the lack of stationarity conditions. However, when the model is evaluated at seasonal scale, by comparing cumulated T_c (as a sum of the daily values in mm), it shows good performances; in fact, it underestimates of − 1% *Olea* and *Pinus* transpiration and overestimates of 8% *Citrus* transpiration.

3.4 Error analysis

The relative error on λT_c was calculated by Eq. (26) where the terms S_a and S_b are the mean of all available values in the experimental period. Error on λT_c due to error in the input parameter a is negligible (data not shown), being between 0 and 1% when the input parameter a varies between 0 and 100% of the experimentally calculated value. The relative error on λT_c due to error in the input parameter b is illustrated in Fig. 9 for both stress and no-stress conditions. For *Pinus*, the error on λT_c is always low, less than 10%; for *Olea*, the error is > 10% when the error on the coefficient b is greater than 50%. For *Citrus*, the error on λT_c is great than 20% when the error on b is greater than 35%.

4 Conclusions

In this study, a transpiration model is presented for three species of urban trees at hourly and daily scales, neglecting the evaporation. The model is based on the PM formula, with the introduction of a semi-empirical parametrization for the canopy resistance. Either at hourly or at daily scale, the canopy resistance is estimated from (i) climatological data and (ii) parameters depending on the species following the plant water status as expressed by the crop water stress index. The species-specific model parameters need experimental calibration.

In this model, canopy resistance is a variable parameter, assuming a specific value at each moment and, consequently, for each day.

The model has been tested in a site of Mediterranean region, under semi-arid climate. On an hourly scale, it seems to work well in contrasting water conditions: when the tree is well watered and under water stress. The performance of the model could be improved by the use of more than two water stress classes; in this case, each interval would be narrow, but the model loses practical applicability.

On a daily scale, the model was not as accurate as at hourly scale giving, however, acceptable estimation of transpiration. It works better at seasonal scale and should be used to determine the trees' water requirements or as output term of urban water balance.

The difficulty in the application of the present model is in the determination of the trees' water status, that here is determined in function of the measured transpiration, which is the

unknown variable. Therefore, further developments are necessary to improve its application especially at daily scale, in particular using estimates of *CWSI* based on surface temperature (Jackson et al. 1981; Stanghellini and De Lorenzi 1994) instead of measurements of transpiration. In fact, an alternative applicative definition of *CWSI* is:

$$CWSI \equiv \frac{T_s - T_m}{T_M - T_m} \quad (27)$$

with T_s surface temperature measurable for example by infrared thermometry, T_m and T_M minimum and maximum tree temperature, respectively, easily calculable by climatological variables (e.g., Stanghellini and De Lorenzi 1994).

Furthermore, Rana et al. (1997b, 2001) for field crops demonstrated that the presented approach does not need a local calibration, like other Penman and PM-based models, but only a "per crop" calibration. If the coefficients "*a*," "*b*," "*A*," and "*B*" of the presented model are known for different crop water conditions, the model would be valid at another site. This hypothesis clearly needs to be verified for trees species in urban environments with further research.

References

Agam N, Cohen Y, Bernic JAJ, Alchanatis V, Kool D, Dag A, Yermiyahu U, Ben-Gal A (2013) An insight to the performance of crop water stress index for olive trees. Agric Water Manag 113:79–86

Allen RG, Pereira LS, Raes D, Smith M (1998) Crop evapotranspiration. Guidelines for computing crop water requirements. Irrigation and Drainage paper No. 56. FAO, Rome, p 300

Amoroso G, Frangi P, Piatti R, Fini A, Ferrini F (2010) Effect of mulching on plant and weed growth, substrate water content, and temperature in container-grown giant arborvitae. HortTechnology 20:957–962

Argov Y, Rössler Y, Voet H, Rosen D (1999) The biology and phenology of the citrus whitefly, Dialeurodes citri, on citrus in the Coastal Plain of Israel. Entomologia Experimentalis et Applicata 93:21–27

Arya SP (2001) Introduction to micrometeorology. Academic Press, London, 420 pp

Asaeda T, Ca VT (1993) The subsurface transport of heat and moisture and its effect on the environment: a numerical model. Bound.-Layer Meteor. 65:159–179

Aubinet M, Vesala T, Papale D (2012) Eddy covariance: a practical guide to measurement and data analysis. Springer, Dordrecht, Heidelberg, London, New York 438 pp

Ballester C, Jiménez-Bello MA, Castel JR, Intrigliolo DS (2013) Usefulness of thermography for plant water stress detection in citrus and persimmon trees. Agric For Meteorol 168:120–129

Ballinas M, Barradas VL (2015) The urban tree as a tool to mitigate the urban heat island in Mexico city: a simple phenomenological model. J. Environ. Qual. https://doi.org/10.2134/jeq2015.01.0056

Barradas VL, Ramos-Vázquez A, Orozco-Segovia A (2004) Stomatal conductance in a tropical xerophilous shrubland at a lava substratum. Int J Biometeorol 48:119–127. https://doi.org/10.1007/s00484-003-0195-x

Ben-Gal A, Agam N, Alchanatis V, Cohen Y, Yermiyahu U, Zipori I, Presnov E, Sprintsin M, Dag A (2009) Evaluating water stress in irrigated olives: correlation of soil water status, tree water status, and thermal imagery. Irrig Sci 27:367–376

Berni JAJ, Zarco-Tejada PJ, Sepulcre-Cantó G, Fereres E, Villalobos F (2009) Mapping canopy conductance and CWSI in olive orchards using high resolution thermal remote sensing imagery. Remote Sens Environ 113:2380–2388

Brutsaert WH (1982) Evaporation into atmosphere: theory, history and application. D. Reidel, Dordrecth, p 299

Čermák J, Kučera J, Nadezhdina N (2004) Sap flow measurements with some thermodynamic methods, flow integration within trees and scaling up from sample trees to entire forest stands. Trees 18:529–546. https://doi.org/10.1007/s00468-004-0339-6

Chen L, Zhang Z, Li Z, Tang J, Caldwell P, Zhang W (2011) Biophysical control of whole tree transpiration under an urban environment in northern China. J Hydrol 402:388–400

Chen L, Zhang Z, Ewers BE (2012) Urban tree species show the same hydraulic response to vapor pressure deficit across varying tree size and environmental conditions. PLoS One 7(10):47882. https://doi.org/10.1371/journal.pone.0047882

Costello LR, Matheny N, Clark J, Jones K (2000) A guide to estimating irrigation water needs of landscape plantings in California. In: The landscape coefficient method and WUCOLS III. University of California Cooperative Extension California Department of Water Resources, Sacramento

Christen A, Vogt R (2004) Energy and radiation balance of a central European city. Int J Climatol 24:1395–1421

Daudet FA, Perrier A (1968) Etude de l'evaporation ou de la condensation a la surface d'un corp a partir du bilan energetique. Rev Gen Therm 76:353–364

Daudet FA, Le Roux X, Sinoquet H, Adam B (1999) Wind speed and leaf boundary layer conductance variation within tree crown consequences on leaf-to-atmosphere coupling and tree functions. Agric. For. Meteorol. 97:171–185

Davies WJ, Metcafle J, Lodge TA, da Costa AR (1986) Plant growth substances and the regulation of growth under drought. Aust J Plant Physiol 13:105–125

Doll D, Ching JKS, Kaneshiro J (1985) Parameterisation of subsurface heating for soil and concrete using net radiation data. Bound.-Layer Meteor. 32:351–372

Doorenbos, J., Kassam, A.H., 1979. Yield response to water. U.N. Food and Agriculture Organization Irrigation and Drainage Paper No. 33, Rome

EEA (European Environment Agency) (2016) Mapping and assessing the condition of Europe's ecosystems: progress and challenges. Report No 3/2016, 148 pp.

Fanjul L, Barradas VL (1985) Stomatal behaviour of two heliophile understorey species of a tropical deciduous forest in Mexico. J Appl Ecol 22:943–954. https://doi.org/10.2307/2403242

Ferrara RM, Mazza G, Muschitiello C, Castellini M, Stellacci AM, Navarro A, Lagomarsino A, Vitti C, Rossi R, Rana G (2017) Short-term effects of conversion to no-tillage on respiration and chemical - physical properties of the soil: a case study in a wheat cropping system in semi-dry environment. Italian Journal of Agrometeorology 1:47–58. https://doi.org/10.19199/2017.1.2038-5625.047

Fini A, Frangi P, Moria J, Donzelli D, Ferrini F (2017) Nature based solutions to mitigate soil sealing in urban areas: results from a 4-year study comparing permeable, porous, and impermeable pavements. Environ Res 156:443–454

Gonzalez-Dugo V, Zarco-Tejada P, Nicolás E, Nortes PA, Alarcón JJ, Intrigliolo DS, Fereres E (2013) Using high resolution UAV thermal imagery to assess the variability in the water status of five fruit tree species within a commercial orchard. Precision Agric 14:660–678

Gonzalez-Dugo V, Zarco-Tejada PJ, Fereres E (2014) Applicability and limitations of using the crop water stress index as an indicator of

water deficits in citrus orchards. Agric For Meteorol 198–199:94–104
Granier A (1985) Une nouvelle méthode pour la mesure du flux de sève brute dans le tronc des arbres. Ann Sci For 42:81–88
Granier A (1987) Mesure du flux de sève brute dans le tronc du Douglas par une nouvelle méthode thermique. Ann Sci For 44:1–14
Grimmond CSB, Oke TR (1991) An evapotranspiration-interception model for urban areas. Water Resour Res 27:1739–1755
Grimmond CSB, Cleugh HA, Oke TR (1991) An objective urban heat storage model and its comparison with other schemes. Atmospheric Environment B 25:311–326
Grimmond CSB, Oke TR (1999) Aerodynamic properties of urban areas derived from analysis of surface form. J Appl Meteorol 38:1262–1292
Holdridge LR, Grenke WC, Hatheway WH, Liang T, Tosi JA (1971) Forest Environments in Tropical Life Zones: a pilot study. Pergamon Press, Oxford.
Hoshika Y, Fares S, Savi F, Gruening C, Goded I, De Marco A, Sicard P, Paoletti E (2017) Stomatal conductance models for ozone risk assessment at canopy level in two Mediterranean evergreen forests. Agric For Meteorol 234–235:212–221
Itier B, Flura D, Belabbes K, Kosuth P, Rana G, Figueiredo L (1992) Relations between relative evapotranspiration and predawn leaf water potential in soybean grown in several locations. Irrig Sci 13:109–114
Jackson RD, Idso SB, Reginato RL, Pinter PJ Jr (1981) Canopy temperature as a crop water stress indicator. Water Resour Res 17:1133–1141
Jarvis PG (1976) The interpretation of the variation in leaf water potential and stomatal conductance found in canopies. Phil Trans R Soc Lond Ser B 273:593–610
Jarvis PG, McNaughton KG (1985) Stomatal control of transpiration: scaling up from leaf to region. Adv Ecol Res 15:1–49
Karlik, J.F., McKay, A.H., (2002). Leaf area index, leaf mass density, and allometric relationships derived from harvest of blue oaks in a California oak savanna. USDA Forest Service Gen. Tech. Rep. PSW-GTR-184
Katerji N, Ferreira I, Mastrorilli N, Losavio N (1990) A simple equation to calculate crop evapotranspiration: results of several years of experimentation. Acta Hortic 278:477–489
Katerji N, Hallaire M (1984) Les grandeurs de reference utilisables dam l'etude de l'alimentation en eau des cultures. Agronomie 4(10):999–1008
Katerji N, Perrier A (1983) Modelisation de l'evapotranspiration reelle d'une parcelle de luzerne: role dune coefficient culturale. Rev Agron 3(6):513–521
Katerji N, Rana G (2011) Crop reference evapotranspiration: a discussion of the concept, analysis of the process and validation. Water Resour Manag 25:1581–1600
Katerji N, Rana G (2013) FAO-56 methodology for determining water requirement of irrigated crops: critical examination of the concepts, alternative proposals and validation in Mediterranean region. Theor Appl Climatol 116(3):515–536
Kelliher FM, Leuning R, Raupach MR, Schulze E-D (1995) Maximum conductances for evaporation from global vegetation types. Agri For Metereol 73:1–16
Kottek M, Grieser J, Beck C, Rudolf B, Rubel F (2006) World map of the Köppen-Geiger climate classification updated. Meteorol Z 15(3): 259–263
Körner C, Scheel JA, Bauer H (1979) Maximum leaf diffusive conductance in vascular plants. Photosynthetica 13(1):45–82
Kreith F (1973) Principle of heat transfer. Dun Donnelley, New York, 651 pp
Legates DR, McCabe GJ (1999) Evaluating the use of 'goodness-of fit' measures in hydrologic and hydroclimatic model validation. Wat Resou Res 35:233–241
Lemonsu A, Grimmond CSB, Masson V (2004) Modeling the surface energy balance of the core of an old Mediterranean city: Marseille. J Appl Met 73:312–327
Lindén J, Fonti P, Espera J (2016) Temporal variations in microclimate cooling induced by urban trees in Mainz. Germany Urb For Urb Gr 20:198–209
Litvak E, McCarthy HR, Pataki DE (2012) Transpiration sensitivity of urban trees in a semi-arid climate is constrained by xylem vulnerability to cavitation. Tree Physiol 32:373–388
Litvak E, McCarthy HR, Pataki DE (2017) A method for estimating transpiration of irrigated urban trees in California. Landsc Urban Plan 158:48–61
Loridan T, Grimmond CSB (2012) Characterization of energy flux partitioning in urban environments: links with surface seasonal properties. Am Meteorol Soc 51:219–241. https://doi.org/10.1175/JAMC-D-11-038.1
McCaughey J (1985) Energy balance storage terms in a mature mixed forest at Petawawa Ontario—a case study. Bound-Layer Meteor 31: 89–101
McNaughton KG (1976) Evaporation and advection. I. Evaporation from extensive homogeneous surfaces. Q J R Meteorol Sot 102:181–191
Mitchell VG, Cleugh HA, Grimmond CSB, Xu J (2008) Linking urban water balance and energy balance models to analyse urban design options. Hydrol Process 22:2891–2900
Monteith JL (1965) Evaporation and atmosphere. The state and movement of water in living organisms. Symposia of the Society for Experimental Biology 19:205–234
Nassar IN, Horton R (1999) Salinity and compaction effects on soil water evaporation and water and solute. Soil Sci Soc Am J 63:752–758. https://doi.org/10.2136/sssaj1999.634752x
Nielsen CN, Bühler O, Kristoffersen P (2007) Soil water dynamics and growth of street and park trees. Arboriculture Urban Forest 33:231–245
Novak, M. D. (1981) The moisture and thermal regimes of a bare soil in the Lower Fraser Valley during spring. Ph.D. thesis, The University of British Columbia, Vancouver, BC, Canada, 153 pp.
Offerle B, Grimmond CSB, Fortuniak K (2005) Heat storage and anthropogenic heat flux in relation to the energy balance of a central European city centre. Int J Climatol 25:1405–1419
Pataki DE, Boone CG, Hogue TS (2011a) Socio-ecohydrology and the urban water challenge. Ecohydrology 347:341–347. https://doi.org/10.1002/eco
Pataki DE, McCarthy HR, Litvak E, Pincetl S (2011b) Transpiration of urban forests in the Los Angeles metropolitan area. Ecol Appl 21(3): 661–677
Perrier A (1975) Etude physique de l'évapotranspiration dans les conditions naturelles. I. evaporation et bilan d'énergie des surface naturelles. Annals of Agronomy, 26, 1–18. II. Expression et paramètres donnant l'évapotranspiration réelle d'une surface mince. Annals of Agronomy, 26, 105–123. III. Evapotranspiration réelle et potentielle des couverts végétaux. Annals of Agronomy 26:229–243 (in French)
Perrier A, Katerji N, Iier B (1980) Etude 'in situ' de l'evapotranspiration reele dune culture de ble. Agric Meteorol 21:295–311
Rana G, Katerji N, Mastrorilli M, El Moujabber M (1994) Evapotranspiration and canopy resistance of grass in a Mediterranean region. Theor Appl Climatol 50(1–2):61–71
Rana G, Katerji N (1998) A measurement based sensitivity analysis of the Penman-Monteith actual evapotranspiration model for crops of different height and in contrasting water status. Theor Appl Climatol 60:141–149
Rana G, Katerji N, Mastrorilli M, El Moujabber M (1997a) A model for predicting actual evapotranspiration under soil water stress in a Mediterranean region. Theor Appl Climatol 56(1–2):45–55

Rana G, Katerji N, Mastrorilli M, El Moujabber M, Brisson N (1997b) Validation of a model of actual evapotranspiration for water stressed soybeans. Agric For Meteorol 86:215–224

Rana G, Katerji N, Mastrorilli M (1997c) Environmental and soil-plant parameters for modelling actual crop evapotranspiration under water stress conditions. Ecol Model 101:363–371

Rana G, Katerji N, Perniola M (2001) Evapotranspiration of sweet sorghum: a general model and multilocal validity in semi arid environmental conditions. Water Resour Res 37(12):3237–3246

Rana G, Katerji N, De Lorenzi F (2005) Measurement and modelling of evapotranspiration of irrigated citrus orchard under Mediterranean conditions. Agric For Meteorol 128(3–4):199–209

Rana G, Katerji N, Lazzara P, Ferrara RM (2012) Operational determination of daily actual evapotranspiration of irrigated tomato crops under Mediterranean conditions by one-step and two-step models: multiannual and local evaluations. Agric Water Manag 115:285–296

Rapisarda, C., Cocuzza, G.E.M. (Eds.), 2017. Integrated pest management in tropical regions. CABI, UK, 359 pp, ISBN 1780648006, 9781780648002

Riikonen A, Järvi L, Nikinmaa E (2016) Environmental and crown related factors affecting street, tree transpiration in Helsinki, Finland. Urban Ecosyst 19:1693–1715. https://doi.org/10.1007/s11252-016-0561-1

Roberts SM, Oke TR, Grimmond CSB, Voogt JA (2006) Comparison of four methods to estimate urban heat storage. J Appl Met Climat 45: 1766–1780

Shi T, Guan D, Wang A, Wu J, Jin C, Han S (2008) Comparison of three models to estimate evapotranspiration for a temperate mixed forest. Hydrol Process 22(17):3431–3443

Shields CA, Tague CL (2012) Assessing the role of parameter and input uncertainty in ecohydrologic modeling: implications for a semi-arid and urbanizing coastal California catchment. Ecosystems 15:775–791. https://doi.org/10.1007/s10021-012-9545-z

Schulze ED (1986) Carbon dioxide and water vapour exchange in response to drought in the atmosphere and in the soil. Ann Rev Plant Physiol 37:247–270

Seidel H, Schunk C, Matiu M, Menzel A (2016) Diverging drought resistance of scots pine provenances revealed by infrared thermography. Frontiers in Plant Science 7:Article 1247. https://doi.org/10.3389/fpls.2016.01247

Spano D, Snyder RL, Sirca C, Duce P (2009) ECOWAT-A model for ecosystem evapotranspiration estimation. Agric For Meteorol 149(10):1584–1596. https://doi.org/10.1016/j.agrformet.2009.04.011

Stanghellini C, De Lorenzi F (1994) A comparison of soil- and canopy temperature-based methods for the early detection of water stress in a simulated patch of pasture. Irrig Sci 14:141–146

Symes P, Connellan G (2013) Water management strategies for urban trees in dry environments: lessons for the future. Arboricult Urban For 39:116–124

Sutanto SJ, Wenninger J, Coenders-Gerrits AMJ, Uhlenbrook S (2012) Partitioning of evaporation into transpiration, soil evaporation and interception: a comparison between isotope measurements and a HYDRUS-1D model. Hydrol Earth Syst Sci 16:2605–2616

Tardieu F, Katrerji N, Bethenod O (1990) Relation entre l'état hydrique du sol, le potentiel de base et d'autres indicateurs del a contrainte hydrique chez le mais. Agronomie 8:617–626

Vahmani P, Hogue TS (2014a) High-resolution land surface modeling utilizing remote sensing parameters and the Noah UCM: a case study in the Los Angeles Basin. Hydrol Earth Syst Sci 18(12): 4791–4806. https://doi.org/10.5194/hess-18-4791-2014

Vahmani P, Hogue TS (2014b) Incorporating an urban irrigation module into the Noah land surface model coupled with an urban canopy model. Journal of Hydrometeorology:140421133412009. https://doi.org/10.1175/JHM-D-13-0121.1

Waldo LI, Schumann AW (2009) Alternative methods for determining crop water status for irrigation of citrus groves. Proc Fla State Hort Soc 122:63–71

Wullschleger SD, Meinzer FC, Vertessy RA (1998) A review of whole-plant water use studies in trees. Tree Physiol 18:499–512

Yoshida A, Tominaga K, Watatani S (1990–91) Field measurements on energy balance of an urban canyon in the summer season. Energy Build. 15–16:417–423